

# GENERIC FABRICATION TECHNOLOGY FOR TRANSPARENT AND SUSPENDED MICROFLUIDIC AND NANOFUIDIC CHANNELS

Thomas S. Hug<sup>1,2</sup>, Thilo Biss<sup>1,3</sup>, Nico F. de Rooij<sup>1</sup> and U. Stauer<sup>1</sup>  
<sup>1</sup> Institute of Microtechnology, Jaquet-Droz 1, 2007 Neuchâtel, Switzerland  
<sup>2</sup> now at Helbling Technik, Hohlstr 614, 8048 Zurich, Switzerland  
<sup>3</sup> now at Biss+Grolimund AG, Kirchgasse 24, 4932 Lotzwil  
e-mail: urs.stauer@unine.ch.

## ABSTRACT

A promising method for fabricating suspended and transparent microfluidic and nanofluidic channels systems made of a thermally grown silicon dioxide is presented. The fabrication is based on the growth of a thermal silicon dioxide in open cavities formed at the interface of two wafers. We demonstrate three different designs of micro- and nanofluidic channels for three applications: 1) Electroosmotic flow measurements through micro- and nanofluidic channel systems were used to estimate the electroosmotic mobility. 2) Resonance measurements on suspended and filled, 100 $\mu\text{m}$  long microchannels were optically performed by using 10x10 $\mu\text{m}$  large, integrated and aluminum coated silicon dioxide mirrors. 3) Hollow cantilevers with a FIB-milled pore at the tip apex were fabricated and used to record scanning force microscopy images.

**Keywords:** Microfluidics, nanofluidics, oscillating channels, suspended channels, scanning force microscopy.

## INTRODUCTION

Silicon dioxide is an excellent material for fluidic systems because of its chemical, optical and electric/isolating properties. We have therefore developed a method for fabricating micro- and nanofluidic systems based on thermally grown  $\text{SiO}_2$ . The basic idea was to oxidize open cavities formed at the interface of

two silicon wafers (Fig. 1). This established chemically well defined surfaces, which are comparable to regular glass capillaries. The high electrical resistivity of thermal silicon dioxide is attractive for electroosmotic pumping. We investigated three different designs of micro- and nanofluidic channels for three applications: Channels with varying cross-section for studying the electroosmotic flow in such channels; suspended channels that could be used for vibration based detection of viscosity; and a free-standing, hair-pin like channel with a tip integrated at the end for scanning force microscopy (SFM) applications. This later application could become attractive for what is known as fountain-pen lithography, where minute amounts of liquid are dispensed by an SFM into a nanometric pattern.[1,2,3]

## FABRICATION

The fabrication of the presented micro- and nanofluidic system was based on four steps (Fig. 1): A) The micro- and nanofluidic channel system was fabricated on the top wafer using photolithography and Si reactive ion etching (RIE). B) The bottom wafer with the fluidic inlets was structured using anisotropic KOH-etching. C) The two wafers were carefully aligned and a thermal oxide in the order of 1  $\mu\text{m}$  thickness was grown. D) The channel system was released using anisotropic KOH etching. Several variations of this process for three applications are illustrated below.

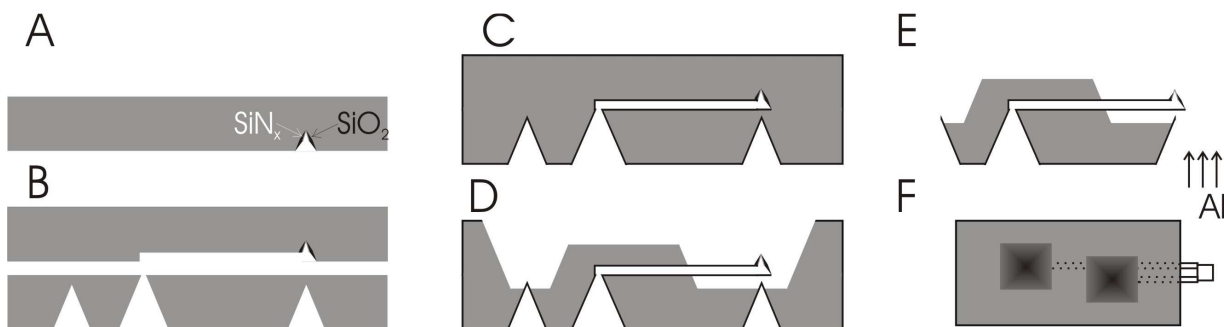


**Fig. 1: Fabrication method illustrated on chips with hollow cantilevers and tips:** A) Top wafer showing the pyramidal etched pits after low temperature oxidation and deposition of a photolithographically structured silicon nitride. B) Top wafer with the cantilevers and the tips and bottom wafer with inlet holes were carefully aligned. C) During wet oxidation a homogeneous silicon dioxide in the order of 1  $\mu\text{m}$  thickness was grown. D) In the next step the silicon dioxide on the backside was photolithographically structured to selectively release the embedded  $\text{SiO}_2$  cantilevers in KOH. E) The chips were manually removed and a 100 nm thick aluminum reflection layer was deposited. F) Top-view of the final chip (1.6x3.6 mm) indicating the inlet and outlet to the microfluidic channel system leading to the cantilevers and the tip.

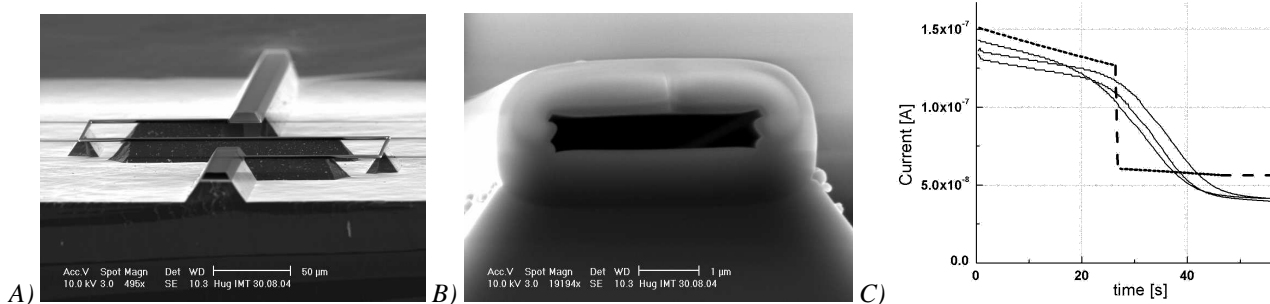


**Fig. 2: Micro- and nanofluidic channels:** A) Slightly tilted micro- and nanofluidic channel system showing a 500  $\mu\text{m}$  long, s-shaped, suspended nanochannel ( $3.5\ \mu\text{m} \times 600\ \text{nm}$ ) and a cleaved microfluidic access channel ( $4.8\ \mu\text{m} \times 19.1\ \mu\text{m}$ ). B) Close-up view of the cross section of a cleaved nanochannel as shown in Fig. 2A. C) EOF measurement through a 300  $\mu\text{m}$  long nanocapillary with buffers of different conductivity to determine the electroosmotic mobility.

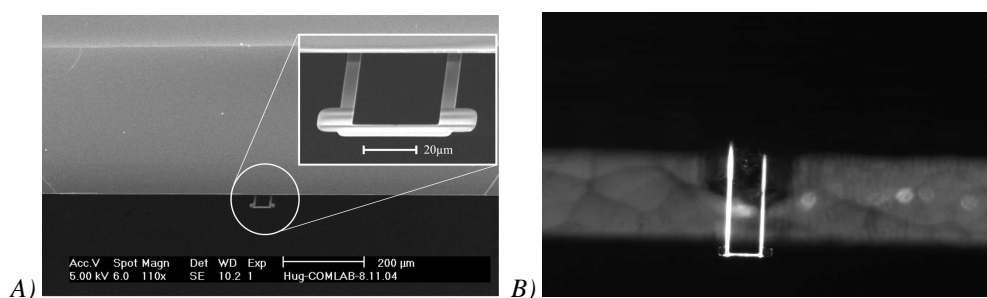


**Fig. 3: Oscillating nanochannels:** A) Front view of a chip with a suspended channel loop having two aluminum coated mirrors for resonance frequency measurements (bottom) and one inlet at the top of the chip (top). Inset shows details of the suspended channel with the mirrors on each side. B) Back view of a chip with a channel loop, filled with a fluorescent solution. Mirrors are barely visible.

## RESULTS AND DISCUSSION

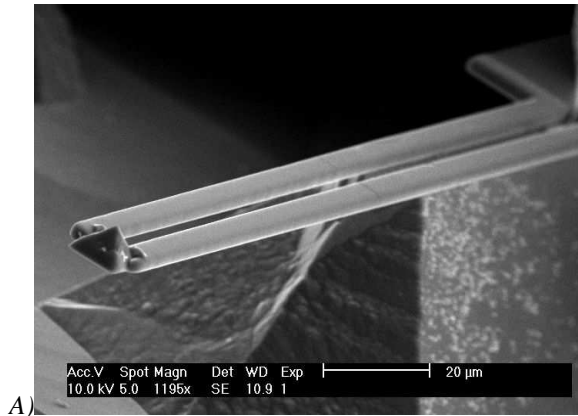
The fabrication of the channels was based on the observation that a uniform oxidation took place inside open channels, formed at the interface between the two wafers, when exposed to an oxidizing atmosphere. There are two phases of oxide growth according to the model of Deal and Grove [4]. Only in the beginning, oxidation is limited by the transport of the oxidizing species in the gas phase. In the second, so called parabolic regime, which is reached within one minute at 1100°C of wet oxidation, the growth of silicon dioxide is limited by the transport of the oxidizing species through the already existing silicon oxide. If the transport of H<sub>2</sub>O vapor through the channels is much faster than through the silicon dioxide, the latter should, hence, homogeneously grow on the full length of the channel. Based on our observation, we conclude that this is the case even for channel cross-sections of less than 300 nm in diameter and a length of several 100  $\mu\text{m}$ . This is demonstrated in the following three examples, where millimeter long microfluidic and nanofluidic channel systems were fabricated by thermal oxidation :

1.) Miniaturization of microfluidic electrophoretic separations in a single nanochannel results in smaller sample volumes, shorter column lengths and separation times. Using our method, 400 microfluidic and

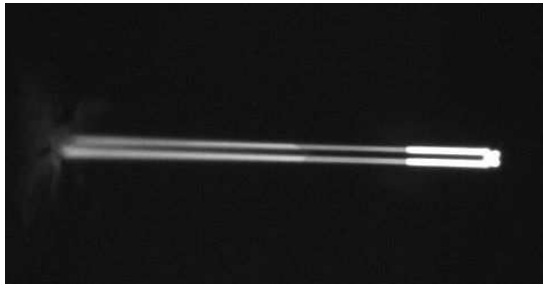
nanofluidic capillaries were fabricated on a single 4 inch wafer (Fig. 2) [5]. Nanochannels were up to one millimeter long and had widths and heights down to 200 nm, whereas microfluidic channels were 20  $\mu\text{m}$  wide and 5  $\mu\text{m}$  high. Depending on the orientation and size, the released channels can be under-etched so that they become freestanding. By designing the resistances of microfluidic access channels and nanochannels a 10 V source was sufficient to reach electrical field strengths up to 600V/cm. Electroosmotic flow measurements with two phosphate buffers having a different conductivity were performed, where electroosmotic mobilities comparable to those in fused silica capillaries were observed (Fig. 2C).

2.) Changes in the resonance frequency of suspended microchannel channel loops were already used by others for biomolecular detection, viscosity-, density- and coriolis-force flow sensors [6,7]. With our method, 120  $\mu\text{m}$  long, resonant microfluidic channels with 1  $\mu\text{m}^2$  cross-section were fabricated (Fig. 3). Depending on the dimensions of empty channels resonance frequencies between 100-300 kHz were measured. Filling of the suspended channels resulted in a resonance frequency shift in the order of 5-70 kHz.

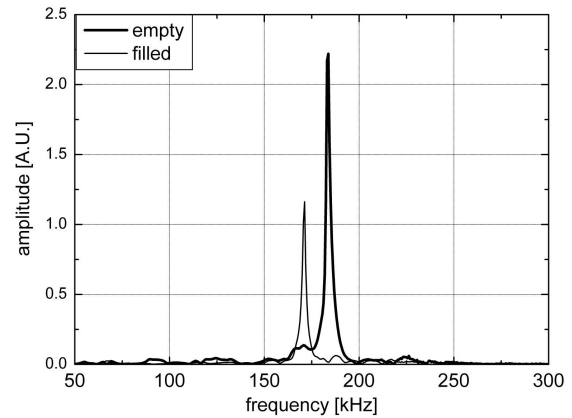
3.) Nanoscale dispensing by means of an AFM tip is an attractive way to pattern various surfaces on the nanometer scale [1-3,8]. A microfluidic channel system integrated in the cantilevers limits the evaporation



A)



B)



C)

**Fig. 4: Cantilevers with tips:** A) SEM picture of a cantilever with integrated tip. B) Microscopic picture of a cantilever filled with fluorescent solution. The end of the cantilevers and the tip appear brighter due to the aluminum coating on the backside. C) Typical resonance frequency measurements of the empty and the filled cantilevers with tips showing the clear resonance frequency shift due to the increased mass.

effects and opens new possibilities to dispense ink not only by capillary forces but also by pressure. Using such feed-channels, also different substances could be dispensed during one writing procedure. Our method was successfully used to fabricate hollow cantilevers with tips all made of a thermally grown silicon dioxide except the tip apex, which is made of silicon nitride (Fig. 4A). Cantilevers were up to 140  $\mu\text{m}$  long and between 4 and 6  $\mu\text{m}$  wide and 3.4  $\mu\text{m}$  high. The fabrication process for the silicon nitride tip apices having a radius of curvature of 200 nm was based on a silicon nitride deposition (low-stress LPCVD  $\text{Si}_x\text{N}_y$ ) after a low temperature oxidation of pyramidal etch-pits. This value can still be improved by at least one order of magnitude as demonstrated in silicon nitride AFM probe fabrication [9]. The measured resonance frequency agreed within the experimental error with the calculated value, based on the measured geometry, i.e. length and cross-section, of the cantilever. Filling of the completely transparent and hydrophilic silicon dioxide cantilevers with an aqueous fluorescent solution resulted in a clear resonance shift, which was correlated to the calculated inner-volume of the hollow cantilever (Fig. 4B,C). Using an oxygen plasma pre-treatment, the pyramidal reservoirs of the two inlets were sealed by tightly bonded PDMS layer. Plastic tubes were connected to the reservoirs through the PDMS seal, such that a hydrostatic pressure of a few 10 mbar could be applied by means of a syringe. This was found to be sufficient for inducing flow from one reservoir through the tip to the second reservoir, where

the level of the liquid could be adjusted by controlling the pressure exerted by the syringe.

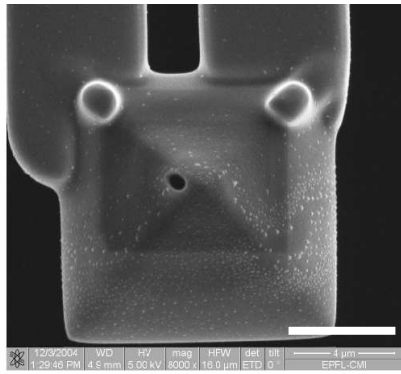
We could also demonstrate, that these probes are suitable for AFM imaging (Fig. 5B). Focused ion beam technique was then used to mill pores between 200nm-2 $\mu\text{m}$  in diameter at the tip, next to its apex for liquid ejection (Fig. 5A), which will be the next experiments to be conducted.

## CONCLUSION

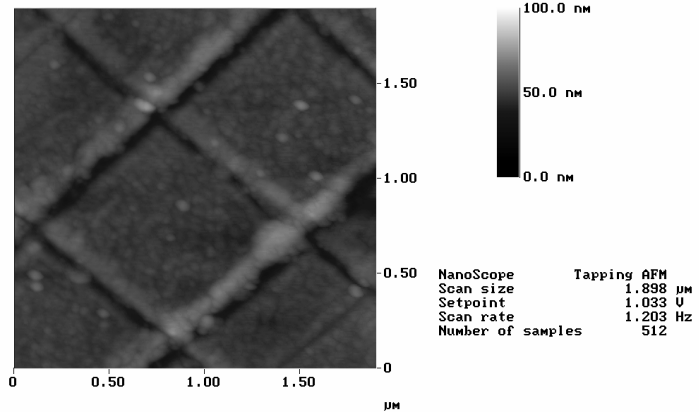
In summary, the presented fabrication approach is not only attractive for making suspended and resonant micro- and nanofluidic sensors, but also for hollow, u-shaped cantilevers and integrated tips for AFM applications. The quality of the thermally grown silicon dioxide proved to be suitable for the electrical field-strengths that are used in electro-osmotic pumping, and mechanically reliable for AFM cantilevers. The process allowed integration of up to 160 AFM-chips, which fit a commercial AFM measuring head, on a single 100 mm wafer.

## Acknowledgements

This work was financed by the Centre Suisse d'Electronique et Microtechnique (CSEM). Helpful discussions with Dr. H. Heinzelmann and Dr. K. Knop from CSEM are gratefully acknowledged. The authors would like to thank the technical staff of ComLab, the joint IMT-CSEM clean room facility, for their support.



A)



B)

**Fig. 5: Focused ion milling and AFM image with a hollow silicon oxide tip:** A) After coating the silicon nitride tips with a 100 nm aluminum layer to reduce charging a focused ion beam was used to mill holes between 200nm up to 2  $\mu\text{m}$  into the tip. The scale bar in the picture is 4 $\mu\text{m}$  long. B) AFM image of a 1 $\mu\text{m}$  calibration grid.

## References

- <sup>1</sup> K.-H. Kim, C. Ke, N. Moldovan, and H.D. Espinosa, Massively parallel multi-tip nanoscale writer with fluidic capabilities – fountain pen nanolithography (FPN), *Proc. 4<sup>th</sup> Internat Symp on MEMS and Nanotechnology*, 235-238 (2003).
- <sup>2</sup> A. Meister, S. Jeney, M. Liley, T. Akiyama, U. Staufer, N.F. de Rooij, and H. Heinzelmann, *Microelectron Eng*, **67-68**, 644-650 (2004).
- <sup>3</sup> S. Deladi, N. R. Tas, J. W. Berenschot, G. J. M. Krijnen, M. J. de Boer, J. H. de Boer, M. Peter, and M. C. Elwenspoek, Micromachined fountain pen for atomic force microscope-based nanopatterning, *Appl. Phys. Lett.* **85**, 5361 (2004).
- <sup>4</sup> B.E. Deal and A.S. Grove, General relationship for thermal oxidation of silicon, *J. Appl. Phys.*, **36**, 12, 3770-3775 (1965).
- <sup>5</sup> T.S. Hug, N.F. de Rooij, U. Staufer, Fabrication and electroosmotic flow measurements in micro- and nanofluidic channels, submitted to *Microfluidics and Nanofluidics*.
- <sup>6</sup> T.P. Burg, S.R. Manalis, Suspended microchannel resonators for biomolecular detection, *Appl. Phys. Lett.*, **83**, 13, 2698-2700 (2003).
- <sup>7</sup> Enoksson P, Stemme G, Stemme E, Silicon tube structures for a fluid-density sensor, *Sensors and Actuators A- Physica*, **54** (1-3): 558-562 (1996).
- <sup>8</sup> D.S. Ginger, et al., The evolution of Dip-Pen Nanolithography, *Angew. Chem. Int. Ed*, **43**, 30-45 (2004).
- <sup>9</sup> S. Akamine, C.F. Quate, Low temperature thermal oxidation sharpening of microcast tips, *J. Vac. Sci. Technol. B*, **10**(5) 2307-2310 (1992).